



Specific inhibitions of annonaceous acetogenins on class II 3-hydroxy-3-methylglutaryl coenzyme A reductase from *Streptococcus pneumoniae*

Lingling Feng^{a,b,*}, Li Zhou^a, Yao Sun^a, Jie Gui^a, Xiaofeng Wang^a, Ping Wu^b, Jian Wan^{a,*}, Yanliang Ren^a, Shengxiang Qiu^b, Xiaoyi Wei^b, Jun Li^c

^a Key Laboratory of Pesticide & Chemical Biology (CCNU), Ministry of Education, College of Chemistry, Central China Normal University, Wuhan 430079, PR China

^b South China Institute of Botany, Chinese Academy of Sciences, Guangzhou 510650, PR China

^c Feed Research Institute, Chinese Academy of Agricultural Sciences, Beijing, 100081, PR China

ARTICLE INFO

Article history:

Received 1 February 2011

Revised 8 April 2011

Accepted 10 April 2011

Available online 20 April 2011

Keywords:

Annonaceous acetogenin

3-Hydroxy-3-methylglutaryl coenzyme A

reductase (class II HMGR)

Inhibition

Streptococcus pneumoniae

Computer modeling and docking simulation

ABSTRACT

3-Hydroxy-3-methylglutaryl coenzyme A reductase (class II HMGR) could serve as a potential target to discover drugs fighting against the invasive diseases originated from *Streptococcus pneumoniae*, one of the major causes of bacterial disease in human. However, no strongly effective inhibitors of class II HMGR have been found so far. In the present study, for the first time, four annonaceous acetogenins (ACGs) were explored for the inhibition on *S. pneumoniae* HMGR. The results showed that the ACGs had higher inhibitory activities against *S. pneumoniae* HMGR with K_i values in the range of 6.45–20.49 μ M than the statin drug lovastatin ($K_i = 116.25 \mu$ M), a classical inhibitor of class I HMGR. Then, three-dimensional modeling and docking simulations analyzed the possible binding mode of ACGs to *S. pneumoniae* HMGR and suggested a kind of novel structural and binding mode for designing promising inhibitor candidates of the targeted enzyme *S. pneumoniae* II HMGR.

© 2011 Elsevier Ltd. All rights reserved.

1. Introduction

Streptococcus pneumoniae is one of the major causes of bacterial disease in human, such as meningitis, septicemia, pneumonia, otitis media and sinusitis. Every year, about 1 million children under 5 years die of the infection of *S. pneumoniae* in developing countries.^{1,2} At the same time, the increasing in strains and antibiotic resistance of *S. pneumoniae* have resulted in more serious problems in conventional antibiotic therapy.^{3–5}

The enzyme 3-hydroxy-3-methylglutaryl coenzyme A reductase (HMGR, EC 1.1.1.34) catalyzes the NAD(P)H-dependent reduction of HMG-CoA to mevalonate, a four-electron oxidoreduction, which is the rate-limiting step in the synthesis of cholesterol and other isoprenoids. HMGRs are found in eukaryotes and prokaryotes, and divided into two classes on the basis of amino

Abbreviation: ACG, annonaceous acetogenin; HMG-CoA, 3-hydroxy-3-methylglutaryl coenzyme A; HMGR, 3-hydroxy-3-methylglutaryl coenzyme A reductase; IPTG, isopropyl β -D-1-thiogalactopyranoside; SDS-PAGE, sodium dodecyl sulfate-polyacrylamide gel electrophoresis; *S. pneumoniae*, *Streptococcus pneumoniae*; THF, tetrahydrofuran.

* Corresponding authors. Tel./fax: +86 27 67862022.

E-mail addresses: flil708@mail.ccnu.edu.cn (L. Feng), jianwan@mail.ccnu.edu.cn (J. Wan).

acid sequences, structure and sensitivity to statins.^{6,7} Characterized class I enzymes include those from human, Syrian hamster, the yeast *Saccharomyces cerevisiae*, the thermophile *Sulfolobus solfataricus* and the halophile *Haloferax volcanii*.^{8–12} In mammals, class I enzyme serves as a critical enzyme for cellular cholesterol synthesis and is strongly inhibited by statin drugs in the nanomolar concentration range, always as the target of the statin class of anti-hypercholesterolemic drugs used to lower cholesterol levels in serum. On the other hand, class II enzymes are utilized by prokaryotes and certain archaea, and have been characterized including those from *Pseudomonas mevalonii*, *Streptomyces* sp., *Staphylococcus aureus*, *S. pneumoniae* and *Archeoglobus fulgidus*.^{13–18} They are less sensitive to statin drugs than class I ones, being inhibited in the micromolar concentration range.¹⁹ HMGR from *S. pneumoniae*, a typical class II HMGR enzyme, could serve as a potential target for drugs fighting against the invasive diseases originated from *S. pneumoniae*, as it acts on an important role during the synthesis of monoterpenes, carotenoids, quinones and membrane components. Up to now, no strongly effective inhibitors of class II HMGR have been reported.

Annonaceous acetogenins (ACGs) are natural products isolated from Annonaceae plants. Due to their novel structure features and broad biological activities which are seldom found in other

natural compounds, ACGs have drawn much attention. Their general structures are characterized by long alkyl chain compounds of 35–37 carbons containing terminal 2,4-disubstituted- γ -lactone, zero to three tetrahydrofuran (THF) rings, and a number of oxygenated moieties (hydroxyls, acetoxy, ketones or epoxides) or double bonds. According to the number and location of THF ring along the hydrocarbon chain, ACGs have been classified into five classes: mono-THF, adjacent bis-THF, non-adjacent bis-THF, tri-THF, non-classical acetogenins (tetrahydropyran and ring-hydroxylated THF ACG).²⁰ ACGs show potent activities by inhibiting NADH-ubiquinone oxidoreductase (complex I) in mitochondrial transport system. They are widely used in pesticidal, antimalarial, antimicrobial, antiparasitic, antiprotozoal, cytotoxic activities and antitumor effects.²¹

In the present study, we found the more potent inhibition of class II HMGR from *S. pneumoniae* by the natural substances ACGs than that by lovastatin, a classical inhibitor of class I HMGR, and analyzed the specific interaction relationship between the ACGs and *S. pneumoniae* HMGR so as to provide detail information for designing the potent inhibitors of class II HMGR based on novel structure features of ACGs.

2. Material and methods

2.1. Materials and reagents

Four ACGs (Fig. 1), squamostatin A, squamostatin B, asimicin and squamocin C, were isolated from the seeds of *Annona squamosa* by Xiao-yi Wei and co-workers (South China Institute of Botany,

Chinese Academy of Sciences) in their previous study.²² The recombinant plasmid pET28-HMGR was kindly provided by Deli Liu (College of life Science, Central China Normal University). Lovastatin, NADPH and HMG-CoA were purchased from Sigma. Other chemicals for the construction, expression of HMGR, protein purification and enzyme assays were purchased from commercial products of analytical grade.

2.2. The expression and purification of *S. pneumoniae* HMGR

The expressing plasmid pET28a-HMGR was transformed into *Escherichia coli* BL21(DE3) and inoculated in Luria-Bertani (LB) broth containing 100 μ g/ml kanamycin at 37 °C reaching a cell density OD₆₀₀ of 0.6–0.8. Then cells were induced with 0.5 mM IPTG for 4 h at 37 °C before harvesting. Purification of the fusion protein was carried out using a Ni²⁺-NTA affinity column attached to an ÄKTA purifier 10 (UPC-F920, GE Healthcare Life Sciences). The concentrations of purified proteins were determined by the method of Bradford²³ using bovine serum albumin (Tiangen) as standard. The final purify (>95%) of the sample was verified by SDS-PAGE and then the purified protein was stored in 50% (v/v) glycerol at 20 °C.

2.3. Enzyme activities and kinetic analysis

Enzymatic assays were performed in a reaction mixture contained 50 mM NaCl, 1 mM EDTA, 25 mM KH₂PO₄, 5 mM DTT, 0.11 μ M enzyme in a final volume of 200 μ l at pH 6.5. For HMG-CoA K_m determination, 0.25 mM NADPH was added and

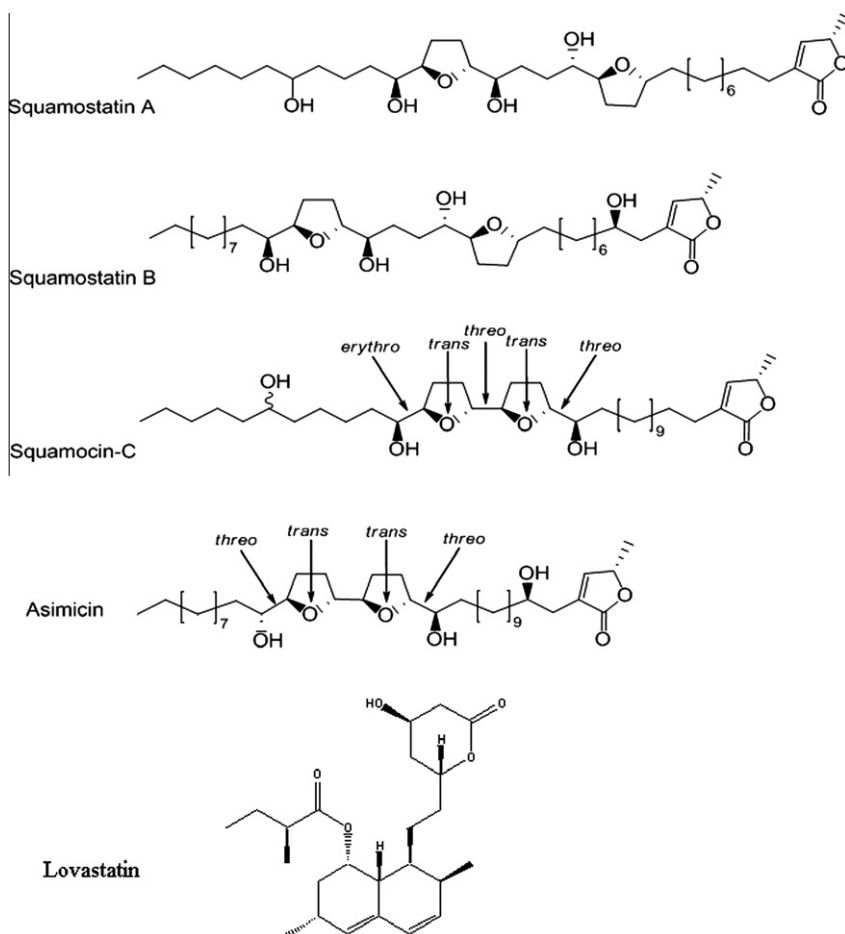


Figure 1. Molecular structures of four ACGs and lovastatin used for study.

the substrate concentration (i.e., HMG-CoA) was varied between 0 and 480 μM . Reactions were at 37 $^{\circ}\text{C}$ for 1 min and the absorbance at 340 nm was monitored in a microplate reader (BioTek Synergy2, USA). The same procedure was utilized for NADPH K_m determination, 100 μM HMG-CoA was added and the substrate concentration (i.e., NADPH) was varied between 0 and 350 μM . For inhibition constant (K_i) determination, a standard reaction mixture contained 50 mM NaCl, 1 mM EDTA, 25 mM KH_2PO_4 , 5 mM DTT, 0.25 mM NADPH, 0.11 μM enzyme, and 20 μM 480 μM HMG-CoA. Increasing concentration of each ACG (ranging from 0 to 50 μM) were incubated for 5 min with HMG-CoA reductase before HMG-CoA added. Kinetic and inhibition constants were determined by non-linear least-squares fitting of the data using the Hill kinetic equations ($v_0 = (V_{\text{max-app}}[S]^n)/(K_{\text{m-app}} + [S]^n)$), where v_0 is the initial velocity, $K_{\text{m-app}}$ is the concentration of substrate eliciting half-maximal velocity, and n is the Hill coefficient in Growth/sigmoidal model from origin 7.0 software.

2.4. Modeling of the three-dimensional structure of *S. pneumoniae* HMGR

SWISSMODEL server (Automated Comparative Protein Modeling Server, Version 3.5, Glaxo Wellcome Experiment Research, Geneva, Switzerland),^{24,25} has been employed to build the homology modeling 3-D structure of HMGR from *S. pneumoniae*. The X-ray crystallographic structural information of HMGR from *P. mevalonii* (PDB ID: 1QAX) was selected as template, which has 42% sequence identity with the target enzyme. The substrate HMG-CoA and NADPH were docked back to the corresponding active site of modeled 3-D structure of HMGR from *S. pneumoniae*, on which all hydrogen atoms were subsequently added to the unoccupied valence of heavy atoms using the BIOPOLYMER mod-

ule of SYBYL 7.0 program package, further energy minimization was also performed using AMBER 8.0 to obtain reasonable structure of HMG-CoA/NADP⁺ complex.

3. Results and discussion

3.1. Expression and purification of *S. pneumoniae* HMGR

The recombinant enzyme was successfully expressed in *E. coli* as a soluble protein after induction by isopropyl β -D-1-thiogalactopyranoside (IPTG). The purity of the recombinant *S. pneumoniae* HMGR was evaluated by sodium dodecyl sulfate–polyacrylamide gel electrophoresis (SDS–PAGE) with the approximately molecular mass 54 kDa as shown in Figure 2. The calculated 6 \times -His-tagged enzyme is 54.3 kDa. The protein was greater than 95% pure by using the criterion of electrophoresis and no discernible degradation. The enzyme was purified to homogeneity by Ni^{2+} -NTA affinity chromatography, yielding 8 mg of pure protein per liter of bacterial culture. The purified enzyme exhibited a specific activity 27.96 μmol of NADPH oxidized $\text{min}^{-1}(\text{mg of enzyme})^{-1}$.

3.2. Kinetic properties of *S. pneumoniae* HMGR

HMGR catalyzes the conversion of HMG-CoA to mevalonate that is the rate-limiting step in the synthesis of cholesterol and other isoprenoids. The optimal pH and temperature of *S. pneumoniae* HMGR for NADPH oxidation was approximately pH 6.5 and 37 $^{\circ}\text{C}$, different from *Listeria monocytogenes* (Fig. 3). *L. monocytogenes* HMGR readily catalyzed HMG-CoA reduction at a pH optimum of 7.0 with NADPH and catalyzed mevalone oxidation at an optimum pH 8.5.²⁶

The catalytic activity of the recombinant HMGR was evaluated by performing enzyme velocity measurements according to the two substrates, HMG-CoA and NADPH. Nonlinear least-squares analysis of the experimental values with respect to the Hill equation yielded that K_m was 75.8 μM with Hill constants of 1.46 for HMG-CoA and 38.88 μM with Hill constants of 1.26 for NADPH. The Hill coefficient values indicated little to no cooperativity of catalytic activity of the recombinant HMG-CoA reductase toward HMG-CoA and NADPH.

Significant similarities as well as differences were apparent upon comparison of *S. pneumoniae* with other previously characterized HMGRs.^{10,12,17,26} As can be seen in Table 1, $K_{\text{m-NADPH}}$ of *S. pneumoniae* HMGR was similar to class II HMGR from *L. monocytogenes*, but was different from class I HMGRs. There was no clearly tendency of $K_{\text{m-HMG-CoA}}$ between class I and class II HMGR. The substrate specific constant (K_{cat}/K_m) showed that *S. pneumoniae* HMGR was five times less efficient using the substrate NADPH than *L. monocytogenes* HMGR.

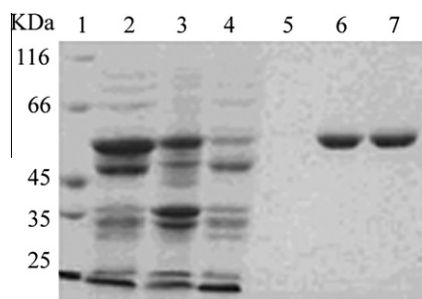


Figure 2. Purification of 6 \times -His-tagged *S. pneumoniae* HMGR. Lane 1: molecular weight standards (kDa). Lane 2: supernatant from induced recombinant cell lysate. Lane 3: precipitate from induced recombinant cell lysate. Lane 4: flowing through. Lane 5: 50 mM imidazole elution. Lanes 6 and 7: 250 mM imidazole elution.

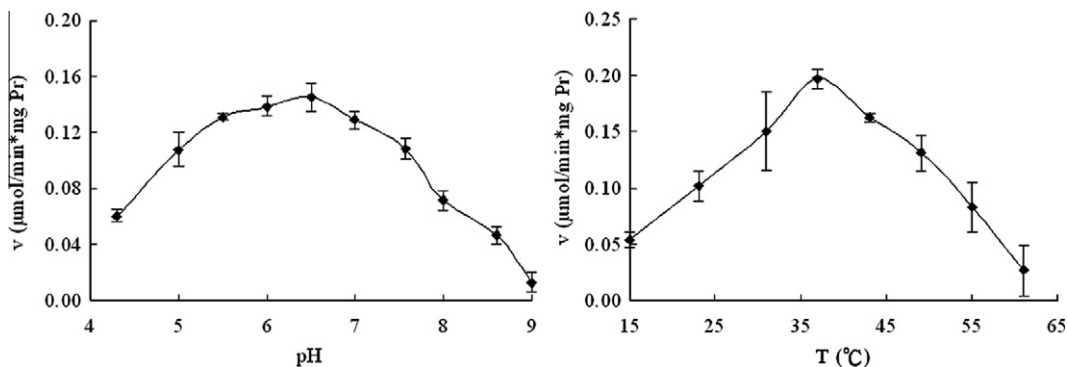
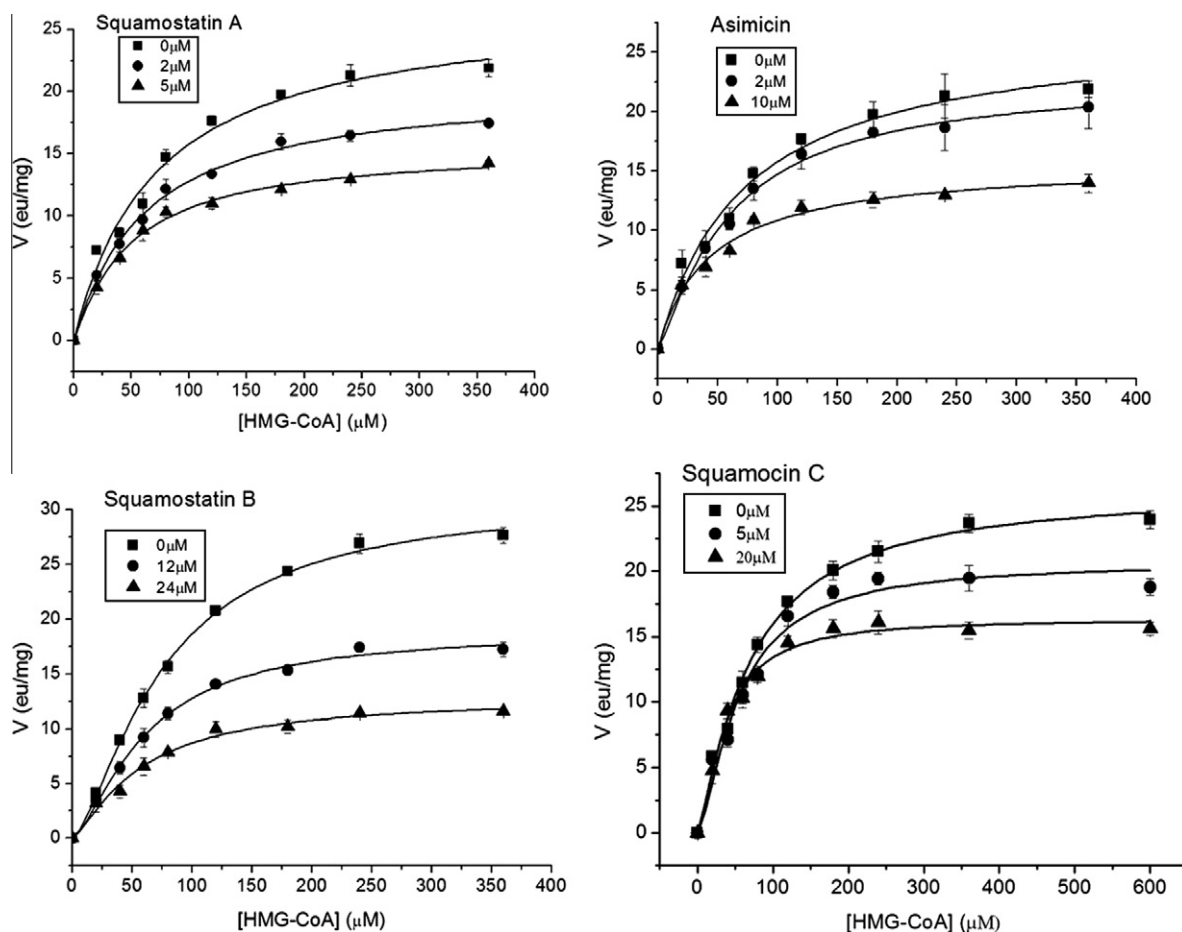


Figure 3. Effects of pH and temperature on enzyme reaction. Enzyme reactions were carried out at different pH (4.3–9) and temperature (15–60 $^{\circ}\text{C}$).

Table 1Kinetic parameters of *S. pneumoniae* HMGR and comparison to representative class I and class II

Variable substrate	<i>Streptococcus pneumoniae</i>	<i>Listeria monocytogenes</i>	<i>Staphylococcus aureus</i>	<i>Haloferax volcanii</i>	Syrian hamster
K_m -HMG-CoA (μM)	75.86 ± 4.43	19.8 ± 1.2	40	60	20
K_m -NADPH (μM)	38.88 ± 4.69	12.9 ± 0.9	70	66	80
k_{cat} -NADPH (S^{-1})	11.95 ± 0.74	22.6			
(k_{cat}/K_m) -NADPH ($\text{S}^{-1} \text{M}^{-1}$)	3.07×105	1.752×106			

**Figure 4.** Effect of ACGs on *S. pneumoniae* HMGR activity. Assays were conducted in the presence of increasing substrate concentration of HMG-CoA in different constant inhibitor concentrations.

3.3. Inhibition of *S. pneumoniae* HMGR by four ACGs

The inhibition constants (K_i) for four ACGs were determined by measuring catalytic activity with an increasing substrate concentration (HMG-CoA) in different constant inhibitor concentrations (Fig. 4). The estimated K_i values were listed in Table 2. Class I HMGR from human has been targeted successfully by statin compounds (f.e. lovastatin) as drugs in the clinical treatment for high serum cholesterol levels, coronary heart disease, anti-inflammation et al.²⁷ But these classical statin drugs have less inhibition to the class II enzyme. ACGs were found to have the higher inhibition potency (6.45 – $20.49 \mu\text{M}$) than lovastatin ($116.25 \mu\text{M}$). The inhibition potency (K_i) of squamostatin A ($6.45 \mu\text{M}$) was nearly 20 times higher than that of lovastatin ($116.25 \mu\text{M}$). Some species were chosen to compare of K_i values.^{15,17,18,26} These results revealed that ACGs have more potent inhibition to class II HMGR than lovastatin, a classical inhibitor of class I HMGR.

3.4. Analysis of *S. pneumoniae* HMGR three-dimensional structure model

An alignment comparing the *S. pneumoniae* HMGR amino acid sequence with other HMG-CoA reductases is shown in Figure 5. Upon alignment with class II HMGRs, the amino acid sequence of

Table 2 K_i of four ACGs to *S. pneumoniae* HMGR and lovastatin to different resource HMGR

	Source	K_i (μM)
Squamostatin A	<i>Streptococcus pneumoniae</i>	6.45 ± 0.22
Asimicin	<i>Streptococcus pneumoniae</i>	12.17 ± 1.70
Squamostatin B	<i>Streptococcus pneumoniae</i>	17.66 ± 1.04
Squamocin C	<i>Streptococcus pneumoniae</i>	20.49 ± 1.89
	<i>Streptococcus pneumoniae</i>	116.25
	<i>Listeria monocytogenes</i>	130
Lovastatin	<i>Staphylococcus aureus</i>	320
	<i>Pseudomonas mevalonii</i>	530
	<i>Archeogiobus fulgidus</i>	180

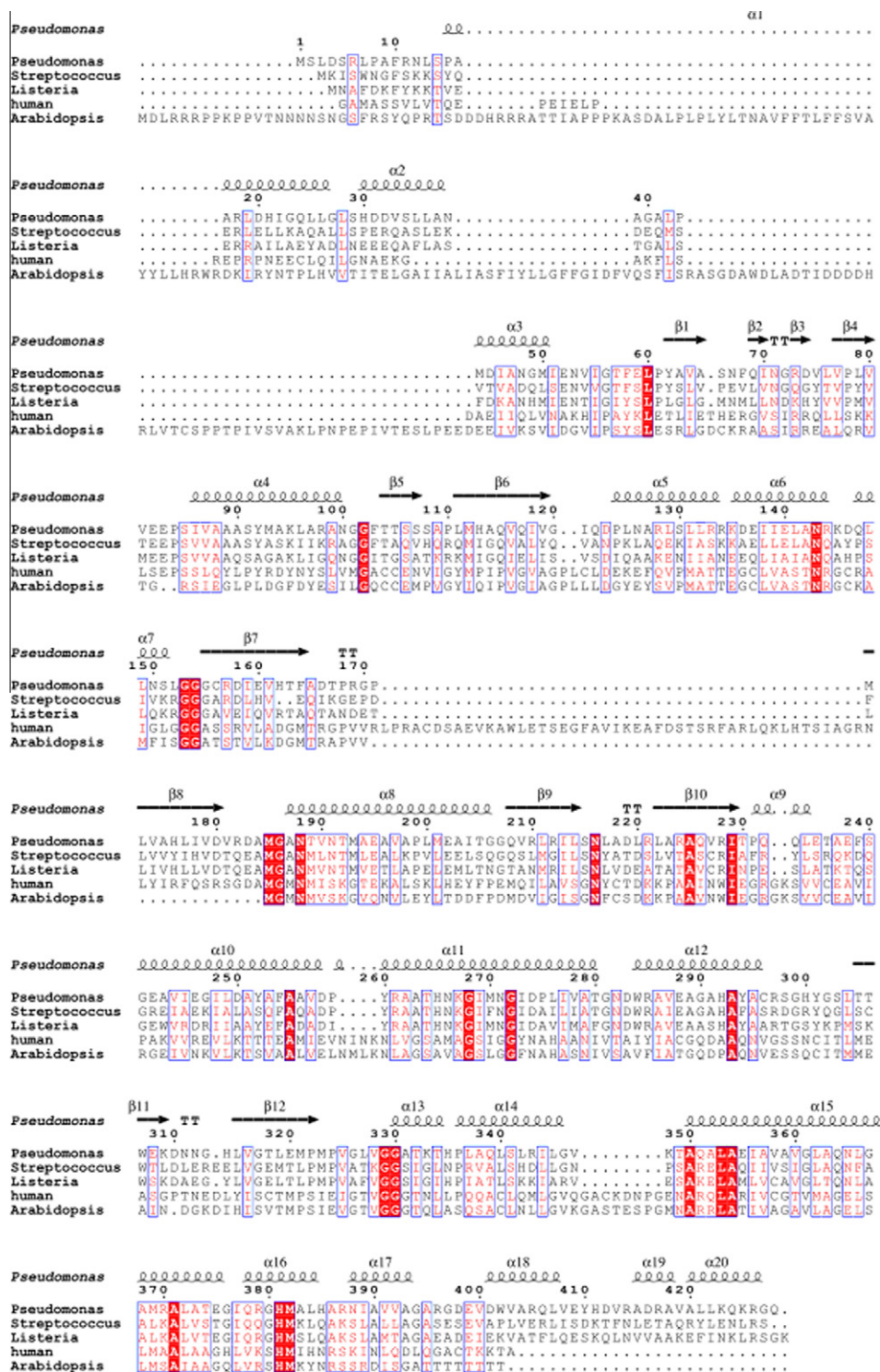


Figure 5. Comparison of the amino acid sequence of *S. pneumoniae* HMGR to other HMGRs.

S. pneumoniae HMGR is 42% identical to *P. mevalonii* HMGR, 47% identical to *L. monocytogenes* HMGR, and 29% identical to *Arabidopsis* HMGR. When compared to class I HMGRs, *S. pneumoniae* HMGR is 23% to human HMGR.

To gain a better understanding of detailed binding models of ACGs, the homology modeling 3-D structure of HMGR from *S. pneumoniae* was obtained using the X-ray crystallographic structural information of HMGR from *P. mevalonii*¹⁴ as template.

The 3-D structural model contained two monomer subunits that form a dimer with two flap domains (Fig. 6A).

The substrates HMG-CoA and NADP⁺ were reasonable docked into the corresponding active site of HMGR from *S. pneumoniae* (Fig. 6A) using SURFLEX module in sybyl7.0. Energy minimization of the final dimeric structure had been performed by using AMBER 8.0 program package to eliminate unfavorable atomic interactions and electrostatic repulsions. Our analysis results revealed that the

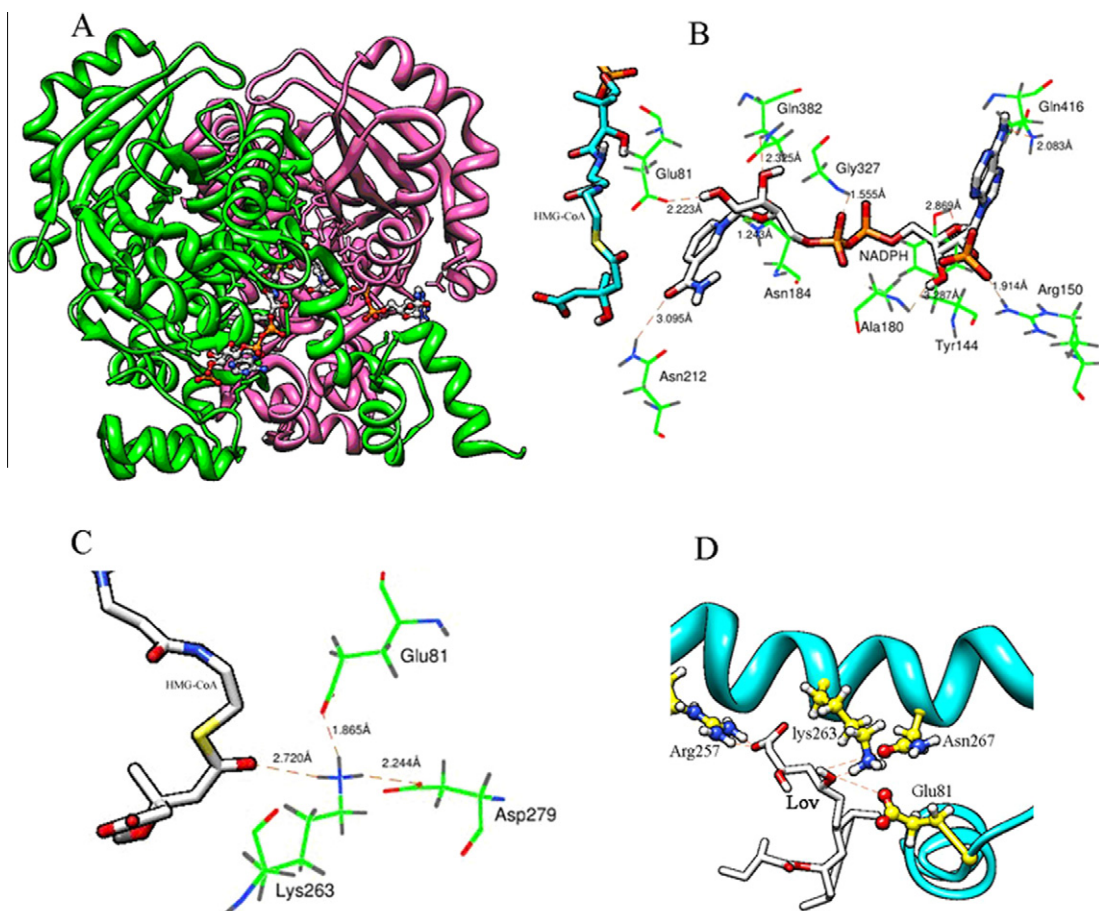


Figure 6. (A) 3D structure model of *S. pneumoniae* HMGR. The polypeptide chain is shown in ribbons and the substrates in spacefill. (B) Interactions at the NADPH (NADP⁺) binding site showing *S. pneumoniae* HMGR residues. (C) Interactions at the HMG-CoA binding site showing *Streptococcus pneumoniae* HMGR residues. (D) Interactions at the lovastatin(Lov) binding site showing *S. pneumoniae* HMGR residues.

putative conserved catalytic residues of HMGR from *S. pneumoniae* were almost identical to that from *P. mevalonii* (Fig. 6B and C) (Table 3). In the HMG-CoA/NADP⁺ complex, the thioester oxygen of HMG-CoA pointed toward the N atom of Lys263. Lys263 was located midway between the substrate and Asp279 which was on the opposite side of Lys263 (Fig. 6C). NADP⁺ had optimal hydrogen bonding with Tyr144, Asn184, Asn212, Glu81, Gly327, Gln382, Ala180, Arg150, and Gln416 (Fig. 6B).

Some studies reported that NADH oxidase assay represents an integrated activity in which NADH is oxidized and the electrons are transferred along the respiratory chain to be finally accepted by molecular oxygen. Therefore, the inhibition of NADH oxidase activity is directly attributed to the inhibition of NADH: ubiquinone oxidoreductase and represents a good method for evaluating the different potency of related compounds.²⁸ ACGs exhibit potent inhibition of bovine complex I only when the two toxophoric moieties are directly linked by the alkyl spacer and cooperatively bind to the two putative binding sites in the Spacer Region of Acetogenins studies.²⁹

The asimicin, squamostatin A, squamostatin B and squamocin C were also docked into the active site occupied by NADP⁺ of HMGR from *S. pneumoniae* (Fig. 7). For these compounds, we found the strong hydrogen bonds interacted with the residues of Tyr144, Asn184, Glu81, Lys263, and Asn212 (Fig. 7) (Table 3). Our docking results also showed that these residues could formate the strong hydrogen bond with cofactor NADP⁺. We therefore suggested that these ACGs compounds possibly take over the place of NADPH,

then block the substrate HMG-CoA to get proton from NADPH, as a result, ACGs strongly inhibit the catalyzed activity of class II HMGR from *S. pneumoniae*. Our model study suggested that four ACGs had more effective inhibition relationship on class II HMGR than lovastatin, possibly due to their binding with NADP⁺ binding sites, not HMG-CoA binding sites.

Previous reports summarized several general conclusions about SAR of ACGs: (i) the adjacent or non-adjacent bis-THF ring ACGs

Table 3
Proposed important amino acid residues for the substrate (HMG-CoA and NADPH), Lovistatin and ACGs binding with *S. pneumoniae* HMGR

	Residues of binding site	K _i (μM)
Squamostatin A	Tyr144, Asn184, Lys263, Glu81, Lys325	6.45 ± 0.22
Asimicin	Tyr144, Asn184, Lys263, Glu81, Lys325	12.17 ± 1.70
Squamostatin B	Gly327, Asn212	
Squamocin C	Tyr144, Asn184, Lys263, Gly327, Asn212, Ser146, Ala180	17.66 ± 1.04
	Tyr144, Asn184, Gly327, Asn212, Ser146, Ala180, Glu416	20.49 ± 1.89
Lovostatin	Lys263, Glu81, Asn267	116.25
NADP ⁺ (NADPH)	Tyr144, Asn184, Glu81, Gly327, Asn212, Ala180, Gln382, Arg150, Gln416	
HMG-CoA	Lys263, Glu81, Asn267	

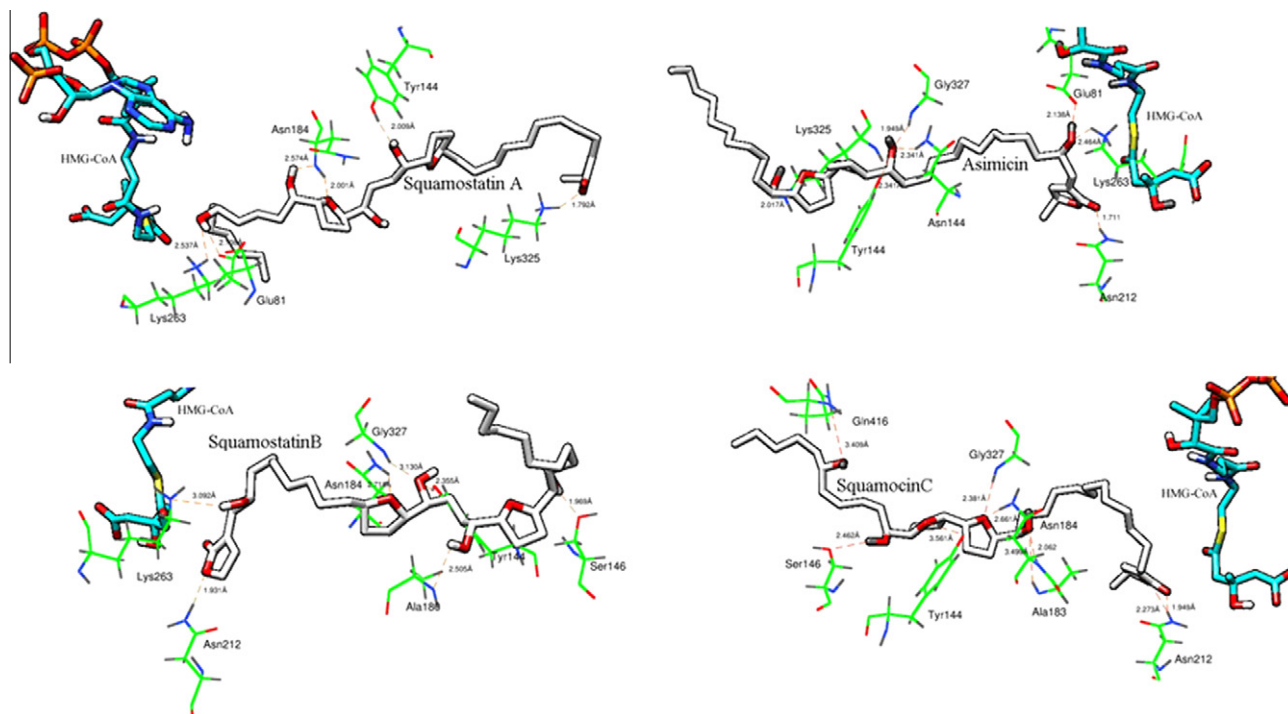


Figure 7. Proposed binding mode for asimicin, squamostatin A, squamostatin B and squamocin C with *S. pneumoniae* HMGR.

showed higher potencies of activity than the mono-THF ring compounds which possessed the same number of hydroxyl groups; and (ii) the potency of activity was related to the number and the positions of the hydroxyl groups and the positions of the THF rings.^{30–33}

With squamostatin A and squamostatin B, four OH groups of different positions existed, two OH groups lied in the long alkyl chain of squamostatin A, also conforming that the position of OH groups could significantly affect the inhibition effects. Especially the OH group in long alkyl chain was better than that by the side of γ -lactone ring. The hydrogen bonds might be the main way that the four ACGs bind with the active pocket of *S. pneumoniae* HMGR. Therefore, the numbers and position of OH groups were of the essence in the enzyme–ACGs interaction.

The various inhibition effects of squamostatin A, squamostatin B and squamocin C indicated that the THF rings possibly play a less important role in the optimum inhibition. Squamocin C belonging to adjacent bis-THF type of ACGs, was less potent against the enzyme than the non-adjacent bis-THF type squamostatin A and squamostatin B, suggesting that the structure of non-adjacent bis-THF ring was more favorable for the inhibition than that of adjacent bis-THF ring, which is inconsistent with the inhibition of NADH oxidase of mitochondrial complex by ACGs.^{32–34}

4. Conclusions

In this report, we have studied the expression, purification, and kinetic characterization of *S. pneumoniae* HMGR and performed the interaction relationship analysis between *S. pneumoniae* HMGR and ACGs. The kinetic characterization revealed that K_m -NADPH of *S. pneumoniae* HMGR was different from class I HMGRs, but there was no clearly tendency of K_m -HMG-CoA between class I and class II HMGR. More importantly, we found that the four ACGs can inhibit *S. pneumoniae* HMGR greater than known classical statin drugs which have potent inhibition on class I HMGR, possibly due to their binding with NADP⁺ binding sites, not HMG-CoA binding sites. The

study suggested a possible kind of novel structural and binding mode for designing promising inhibitor candidates of the targeted enzyme *S. pneumoniae* II HMGR. A potential future research would employ site-directed mutagenesis and computer-aided drug design (CADD) to design and discover better drugs than the classical statins to fight against the invasive diseases originated from *S. pneumoniae*.

Acknowledgments

We thank Prof. Deli LIU for kindly providing the plasmid pET28-HMGR. This work was supported by the Natural Science Foundation of China (Nos. 20672041, 20873049, 20872044 and 21072073), the National Basic Research Program of China (Nos. 2010CB126103, 2007CB116302), the Program for New Century Excellent Talents in University of China (NCET-06-0673), the PCSIRT (No. IRT0953), self-determined research funds of CCNU from the colleges' basic research and operation of MOE (Nos. CCNU09A01010, CCNU10C01002, and CCNU10A02006), the Program for Academic Leader in Wuhan Municipality (No. 201150530150), the Open Project Program of Key Laboratory of Feed Biotechnology of the Ministry of Agriculture of the People's Republic of China.

References and notes

- Brown, S. D.; Rybak, M. J. *J. Antimicrob. Chemother.* **2004**, *54*, 7.
- Garenne, M.; Rosmans, C.; Campbell, H. *World Health Stat.* **1995**, *46*, 180.
- Ubukata, K.; Chiba, N.; Hasegawa, K.; Kobayashi, R.; Iwata, S.; Sunakawa, K. *Antimicrob. Agents Chemother.* **2004**, *48*, 1488.
- Chiba, N.; Kobayashi, R.; Hasegawa, K.; Morozumi, M.; Nakayama, E.; Tajima, T. *J. Antimicrob. Chemother.* **2005**, *56*, 756.
- Hangjia, C.; Chijia, Z.; Jianqiao, P. *Med. Lab. Sci. Clin.* **2007**, *118*, 38.
- Bochar, D. A.; Stauffacher, C. V.; Rodwell, V. W. *Mol. Genet. Metab.* **1999**, *66*, 122.
- Bochar, D. A.; Brown, J. R.; Doolittle, W. F.; Klenk, H. P.; Lam, W.; Schenk, M. E.; Stauffacher, C. V.; Rodwell, V. W. *J. Bacteriol.* **1997**, *179*, 3632.
- Tabernero, L.; Bochar, D. A.; Rodwell, V. W.; Stauffacher, C. V. *Proc. Natl. Acad. Sci.* **1999**, *96*, 7167.

9. Mayer, R. J.; Debouck, C.; Metcalf, B. W. *Arch. Biochem. Biophys.* **1988**, *26*, 110.
10. Frimpong, K.; Darnay, B. G.; Rodwell, V. W. *Prot. Expr. Purif.* **1993**, *4*, 337.
11. Basson, M. E.; Thorsness, M.; Rine, J. *Proc. Natl. Acad. Sci.* **1986**, *83*, 5563.
12. Bischoff, K. M.; Rodwell, V. W. *J. Bacteriol.* **1996**, *178*, 19.
13. Jordan, S. T. C.; Rodwell, V. W. *J. Biol. Chem.* **1989**, *264*, 17913.
14. Friesen, J. A.; Rodwell, V. W. *Genome Biol.* **2004**, *5*, 248.1.
15. Beach, M. J.; Rodwell, V. W. *J. Bacteriol.* **1989**, *171*, 2994.
16. Takahashi, S.; Kuzuyama, T.; Seto, H. *Bacteriology* **1999**, *181*, 1256.
17. Wilding, E. I.; Kim, D. Y.; Bryant, A. P.; Gwynn, M. N.; Lunsford, R. D.; McDevitt, D.; Myers, J. E.; Rosenberg, M.; Sylvester, D.; Stauffacher, C. V.; Rodwell, V. W. *J. Bacteriol.* **2000**, *182*, 5147.
18. Kim, D. Y.; Ryu, S. Y.; Lim, J. E.; Lee, Y. S.; Ro, J. Y. *Eur. J. Pharmacol.* **2007**, *557*, 76.
19. Hedl, M.; Tabernero, L.; Stauffacher, C. V.; Rodwell, V. W. *J. Bacteriol.* **2004**, *186*, 1927.
20. Alali, F. Q.; Liu, X. X.; McLaughlin, J. L. *J. Nat. Prod.* **1999**, *62*, 504.
21. Fang, X. P.; Rieser, M. J.; Gu, Z. M.; Zhao, G. X.; McLaughlin, J. L. *Phytochem. Anal.* **1993**, *4*, 27.
22. Xie, H. H.; Wei, X. Y.; Wang, J. D.; Liu, M. F.; Yang, R. Z. *Chin. Chem. Lett.* **2003**, *14*, 588.
23. Bradford, M. M. *Anal. Biochem.* **1976**, *72*, 248.
24. Schwede, T.; Kopp, J.; Guex, N.; Peitsch, M. C. *Nucleic Acids Res.* **2003**, *31*, 3381.
25. Guex, N.; Peitsch, M. C. *Electrophoresis* **1997**, *18*, 2714.
26. Theivag, A. E.; Amanti, E. A.; Beresford, N. J.; Tabernero, L.; Friesen, J. A. *Biochemistry* **2006**, *45*, 14397.
27. Tousoulis, D.; Charakida, M.; Stefanadi, E.; Siasos, G.; Latsios, G.; Stefanadis, C. *Int. J. Cardiol.* **2007**, *115*, 144.
28. Degli, E. M.; Ghelli, A.; Ratta, M.; Cortes, D.; Estornell, E. *Biochem. J.* **1994**, *301*, 161.
29. Abe, M.; Kubo, A.; Yamamoto, S.; Hatoh, Y.; Abe, M.; Kubo, A. *Biochemistry* **2008**, *47*, 6260.
30. Abe, M.; Kenmochi, A.; Ichimaru, N.; Hamada, T.; Nishioka, T.; Miyoshi, H. *Bioorg. Med. Chem. Lett.* **2004**, *149*, 779.
31. Xu, Z. F.; Wei, X. Y.; Xie, H. H.; Yang, R. Z. *Biol. Pharm. Bull.* **2003**, *26*, 729.
32. Miyoshi, H.; Ohshima, M.; Shimada, H.; Akagi, T.; Iwamura, H.; McLaughlin, J. C. *Biochim. Biophys. Acta* **1998**, *1365*, 443.
33. He, K.; Zeng, L.; Ye, Q.; Shi, G. E.; Oberlies, N. H.; Zhao, G. X.; Njoku, C. J.; McLaughlin, J. L. *Pestic. Sci.* **1997**, *49*, 372.
34. Gallardo, T.; Saez, J.; Granados, H.; Tormo, J. R.; Velez, I. D. *J. Nat. Prod.* **1999**, *2*, 1001.